Article

Receptor for Anionic Pyrene Derivatives Provides the Basis for New Biomembrane Assays

Christine A. Winschel, Amar Kalidindi, Ibrahim Zgani, John L. Magruder, and Vladimir Sidorov

J. Am. Chem. Soc., **2005**, 127 (42), 14704-14713• DOI: 10.1021/ja052397i • Publication Date (Web): 27 September 2005

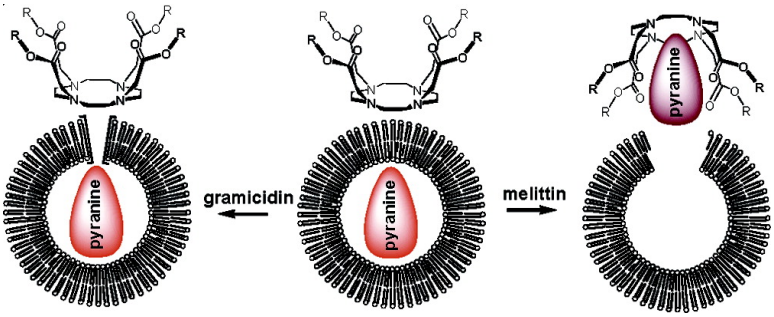

More About This Article

Additional resources and features associated with this article are available within the HTML version:

- Supporting Information
- Links to the 3 articles that cite this article, as of the time of this article download
- Access to high resolution figures
- Links to articles and content related to this article
- Copyright permission to reproduce figures and/or text from this article

View the Full Text HTML

J|A|C|S
ARTICLES
Published on Web 09/27/2005

Receptor for Anionic Pyrene Derivatives Provides the Basis for New Biomembrane Assays

Christine A. Winschel, Amar Kalidindi, Ibrahim Zgani, John L. Magruder, and Vladimir Sidorov*

Contribution from the Department of Chemistry, Virginia Commonwealth University, Richmond, Virginia 23284-2006

Received April 13, 2005; E-mail: vasidorov@vcu.edu

Abstract: This study describes a new receptor cyclen **1** capable of strong selective binding of pyrene-based anionic dyes under near-physiological conditions. This receptor comprises four naphthylthiourea groups tethered to a cyclen core via an ester linkage. The complexation behavior of cyclen **1** receptor is characterized by a series of ^{1}H NMR, microcalorimetry, UV−vis, and fluorometry experiments. The relevance of structural features of this receptor to its recognition function is assessed using control compounds that lack some of the groups found in cyclen **1**. The specificity of cyclen **1** toward pyrene-based dyes is assessed through experiments using dyes with different molecular organization. The most important finding was the ability of cyclen **1** to bind efficiently to a pH-sensitive dye pyranine, a dye that is commonly used in various biomembrane assays. The high affinity of cyclen **1** to pyranine, its impermeability to the lipid bilayer membrane, fast kinetics of binding, and ability to quench the pyranine's fluorescence were used as a basis for a new membrane leakage assay. This membrane leakage assay is fully compatible with the commonly applied pH-stat transport assay, and therefore it allows for differentiation of the ion transport and nonselective leakage mechanisms within a single set of experiments. The ability of cyclen **1** to quench the fluorescence of pyranine also finds limited applicability to the detection of endovesiculation.

Introduction

Synthetic ionophores[1] have shown promise as a basis for new antibiotics,[2] therapeutics for genetic diseases,[3] sensors,[4] and enzyme mimetics.[5] As a result, there is a growing need for the development of assays to rapidly assess the activity of such compounds under near-physiological conditions.

Along with ^{23}Na NMR[6] and planar bilayer voltage-clamp[7] (PBVC) experiments, the liposome-based pH-stat fluorometric assay is an assay routinely used for identification of physiologically relevant ionophores (Chart 1A).[8] In this assay, a controlled amount of the base and potential ionophore is added to a suspension of liposomes containing a pH-sensitive dye, 8-hydroxypyrene-1,3,6-trisulfonate (HPTS, pyranine),[9] or sometimes fluorescein.[10] The resulting pH gradient across the bilayer membrane causes the efflux of hydronium ions and builds up an electrostatic potential. This potential can be compensated by the efflux of anions or influx of cations. If the compound of interest mediates such ion transport, the efflux of hydronium ions continues altering the intravesicular pH and the fluorescence

(1) Matile, S.; Som, A.; Sorde, N. *Tetrahedron* **2004**, *60*, 6405−6435.
(2) (a) Fernandez-Lopez, S.; Kim, H. S.; Choi, E. C.; Delgado, M.; Granja, J. R.; Khasanov, A.; Kraehenbuehl, K.; Long, G.; Weinberger, D. A.; Wilcoxen, K. M.; Ghadiri, M. R. *Nature* **2001**, *412*, 452−455. (b) Leuschner, C.; Hansel, W. *Curr. Pharm. Des.* **2004**, *10*, 2299−2310. (c) Meyer, A. E.; Leevy, W. M.; Pajewski, R.; Suzuki, I.; Weber, M. E.; Gokel, G. W. *Bioorg. Med. Chem.* **2005**, *13*, 3321−3327. (d) Leevy, W. M.; Weber, M. E.; Schlesinger, P. H.; Gokel, G. W. *Chem. Commun.* **2005**, 89−91.
(3) (a) Sidorov, V.; Kotch, F. W.; Kuebler, J. L.; Lam, Y.-F.; Davis, J. T. *J. Am. Chem. Soc.* **2003**, *125*, 2840−2841. (b) Sidorov, V.; Kotch, F. W.; Abdrakhmanova, G.; Mizani, R.; Fettinger, J. C.; Davis, J. T. *J. Am. Chem. Soc.* **2002**, *124*, 2267−2278. (c) Deng, G.; Dewa, T.; Regen, S. L. *J. Am. Chem. Soc.* **1996**, *118*, 8975−8976. (d) Jiang, C.; Lee, E. R.; Lane, M. B.; Xiao, Y.-F.; Harris, D. J.; Cheng, S. H. *Am. J. Physiol.* **2001**, *281*, L1164−L1172.
(4) (a) Descalzo, A. B.; Rurack, K.; Weisshoff, H.; Martinez-Manez, R.; Marcos, M. D.; Amoros, P.; Hoffmann, K.; Soto, J. *J. Am. Chem. Soc.* **2005**, *127*,184−200. (b) Cornell, B. A.; Braach-Maksvytis, V. L. B.; King, L. G.; Osman, P. D. J.; Raguse, B.; Wieczorek, L.; Pace, R. J. *Nature* **1997**, *387*, 580−583. (c) Litvinchuk, S.; Sorde, N.; Matile, S. *J. Am. Chem. Soc.* **2005**, *127*, 9316−9317.
(5) (a) Sasaki, Y.; Shukla, R.; Smith, B. D. *Org. Biomol. Chem.* **2004**, *2*, 214−219. (b) Baumeister, B.; Matile, S. *Macromolecules* **2002**, *35*, 1549−1555. (c) Som, A.; Matile, S. *Eur. J. Org. Chem.* **2002**, *22*, 3874−3883. (d) Baumeister, B.; Sakai, N.; Matile, S. *Org. Lett.* **2001**, *3*, 4229−4232.
(6) (a) Riddell, F. G.; Hayer, M. K. *Biochim. Biophys. Acta* **1985**, *817*,313−317. (b) Riddell, F. G.; Arumugam, S. *Biochim. Biophys. Acta* **1989**, *984*, 6−10. (c) Bandyopadhyay, P.; Janout, V.; Zhang, L. H.; Sawko, J. A.; Regen, S. L. *J. Am. Chem. Soc.* **2000**, *122*, 12888−12889. (d) Bandyopadhyay, P.; Janout, V.; Zhang, L. H.; Regen, S. L. *J. Am. Chem. Soc.* **2001**, *123*, 7691−7696. (e) Zhang, J. B.; Jing, B. W.; Regen, S. L. *J. Am. Chem. Soc.* **2003**, *125*, 13984−13987.
(7) (a) Eggers, P. K.; Fyles, T. M.; Mitchell, K. D. D.; Sutherland, T. *J. Org. Chem.* **2003**, *68*, 1050−1058. (b) Gokel, G. W. *Cell Biochem. Biophys.* **2001**, *35*, 211−231. (c) Ishida, H.; Qi, Z.; Sokabe, M.; Donowaki, K.; Inoue, Y. *J. Org. Chem.* **2001**, *66*, 2978−2989. (d) Kobuke, Y.; Nagatani, T. *J. Org. Chem.* **2001**, *66*, 5094−5101.
(8) Fyles, T. M.; James, T. D.; Kaye, K. C. *J. Am. Chem. Soc.* **1990**, *115*, 12315−12321.
(9) Pyranine is preferred due to the pK_a value complying with the physiological pH range and two distinct excitation maxima found for its protonated and deprotonated forms. The ratiometric monitoring of pH using these two excitation maxima makes the observed response independent from pyranine concentration: (a) Kano, K.; Fendler, J. H. *Biochim. Biophys. Acta* **1978**, *509*, 289−299. For some recent examples of pyranine-based pH-stat transport assays see: (b) Jeon, Y. J.; Kim, H.; Jon, S.; Selvapalam, N.; Oh, D. H.; Seo, I.; Park, C. S.; Jung, S. R.; Koh, D. S.; Kim, K. *J. Am. Chem. Soc.* **2004**, *126*, 15944−15945. (c) Iwaszko, E.; Wardak, A.; Krupa, Z.; Gruszecki, W. I. *J. Photochem. Photobiol. B* **2004**, *74*, 13−21. (d) Coutinho, A.; Silva, L.; Fedorov, A.; Prieto, M. *Biophys. J.* **2004**, *87*, 3264−3276.
(10) Carmichael, V. E.; Dutton, P. J.; Fyles, T. M.; James, T. D.; Swan, J. A.; Zojaji, M. *J. Am. Chem. Soc.* **1989**, *111*, 767−768.

10.1021/ja052397i CCC: $30.25

Chart 1. (A) pH-Stat Experiment;[a] (B) Membrane Leakage Assay;[b] (C) Endovesiculation Detection

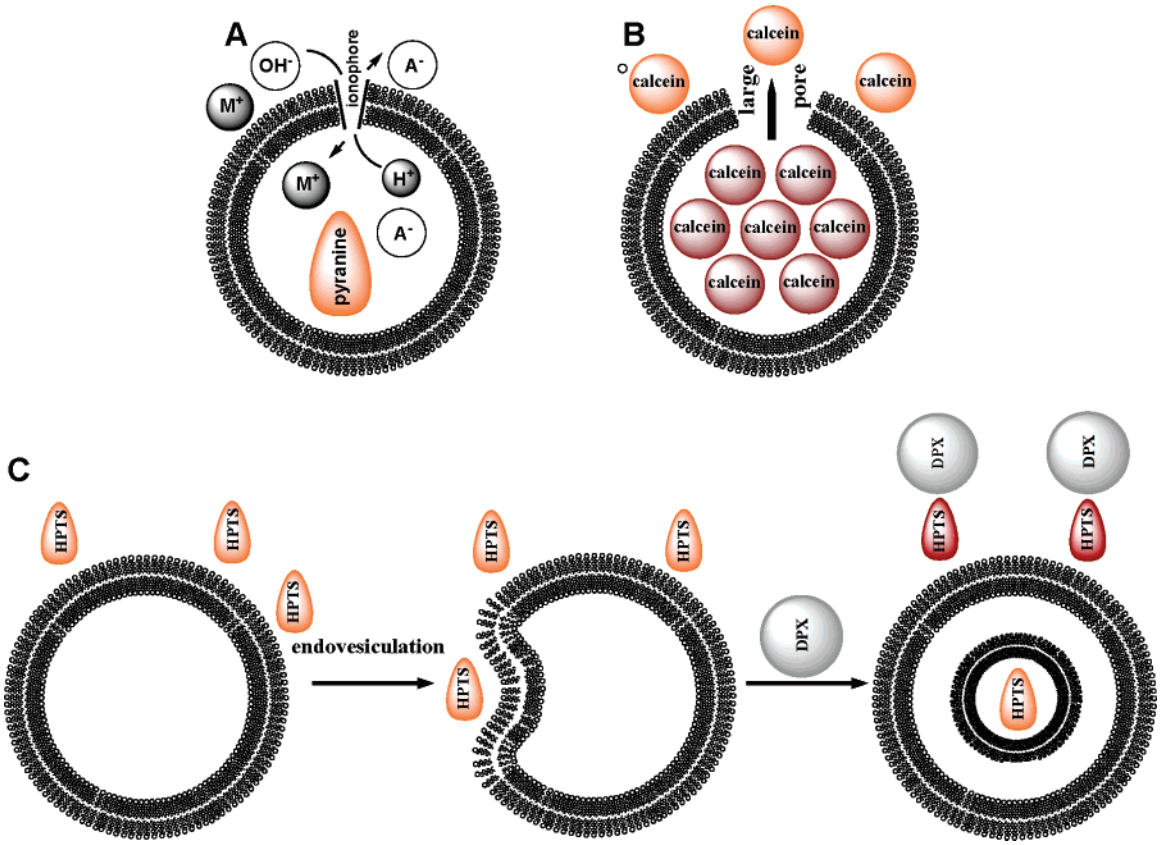

[a] The fluorescence of the pH-sensor pyranine in liposomes is monitored as a function of time; the H^+ release is a result of exogenous application of the base and ionophore. [b]LUVs containing calcein are probed with the ionophore. In the case of large pore formation, the self-quenching dye is released and restores the emission. [c]Liposomes are incubated with pyranine and endovesiculogen, followed by the fluorescence quenching with DPX; the residual fluorescence of entrapped dye serves as a measure of endovesiculation extent.

of the reporter dye. The kinetic trace obtained from the dye response thus reflects the ionophoretic activity of the studied compound. While being rapid and reliable, the pH-stat assay provides little information on the mechanism of ion transport.[11] PBVC provides mechanistic information in high detail;[11] however, it often lacks reproducibility and requires specific skills and extensive time investment.[7b,12] The results of pH-stat and PBVC experiments do not necessarily correlate due to the difference in membrane models and experimental conditions.[12,13]

A membrane leakage assay addresses some mechanistic aspects by distinguishing selective ion transport from nonselective leakage through oversized pores (Chart 1B).[14] This assay utilizes the ability of calcein or carboxyfluorescein (CF) dyes to self-quench their fluorescence emission at ~100 mM concentration. In a typical experiment, a set of large unilamellar vesicles (LUVs) containing the concentrated dye is challenged with the compound of interest. In the case of selective ion transport, little change in fluorescence is observed, whereas the larger pore formation results in the dye release, its subsequent dilution, and emission increase. However, whereas the pH-stat assay is based on LUVs containing the dye at low concentration (100 μM), the high concentration of the dye in leakage assays (100 mM) could alter the membrane properties, change the buffer capacity, and interact with the ionophore. For optimal compatibility and reliability, the same LUVs should be utilized in both pH-stat and membrane leakage assays.

As one of the reviewers pointed out, a similar problem exists with an assay applied to the detection of the endovesiculation process, a mechanistic analogue of cellular endocytosis.[15] Endovesiculation is detected through the incubation of liposomes with exogenous pyranine and endovesiculogen, followed by the quench of extravesicular dye with the membrane-impermeable dynamic quencher *p*-xylene-bis-pyridinium bromide (DPX) at 40 mM concentration (Chart 1C). The portion of the dye entrapped during endovesiculation is inaccessible to the quencher and remains fluorescent. This residual fluorescence serves as a measure of the endovesiculation extent. It has been reported that DPX affects the fluidity of negatively charged membranes, alters the size of LUVs, and lowers the bilayer phase transition temperatures at millimolar concentrations.[16] To avoid all these artifact events and misinterpretations of results, a fluorescence quencher operating at much lower concentration than currently used DPX is required for endovesiculation detection.

(11) Gokel, G. W.; Schlesinger, P. H.; Djedovic, N. K.; Ferdani, R.; Harder, E. C.; Hu, J. X.; Leevy, W. M.; Pajewska, J.; Pajewski, R.; Weber, M. E. *Bioorg. Med. Chem.* **2004**, *12*, 1291−1304
(12) (a) Cameron, L. M.; Fyles, T. M.; Hu, C.-W. *J. Org. Chem.* **2002**, *67*, 1548−1553. (b) Fyles, T. M.; Knoy, R.; Mullen, K.; Sieffert, M. *Langmuir* **2001**, *17*, 6669−6674.
(13) Sakai, N.; Houdebert, D.; Matile, S. *Chem. Eur. J.* **2003**, *9*, 223−232.
(14) (a) Rex, S. *Biophys. Chem.* **1996**, *58*, 75−85. (b) Barbet, J.; Machy, P.; Truneh, A.; Leserman, L. D. *Biochim. Biophys. Acta* **1984**, *772*, 347−356.
(15) (a) Tedesco, M. M.; Matile, S. *Bioorg. Med. Chem.* **1999**, *7*, 1373−1379. (b) Matsuo, H.; Chevallier, J.; Mayran, N.; Le Blanc, I.; Ferguson, C.; Faure, J.; Blanc, N. S.; Matile, S.; Dubochet, J.; Sadoul, M.; Parton, R. G.; Vilbois, F.; Gruenberg, J. *Science* **2004**, *303*, 531−534.
(16) Walter, A.; Siegel, D. P. *Biochemistry* **1993**, *32*, 3271−3281.

Chart 2. (A) Compounds Used in the Present Study; (B) Envisioned Binding Mode for Cyclen **1** and Pyranine Dye[a]

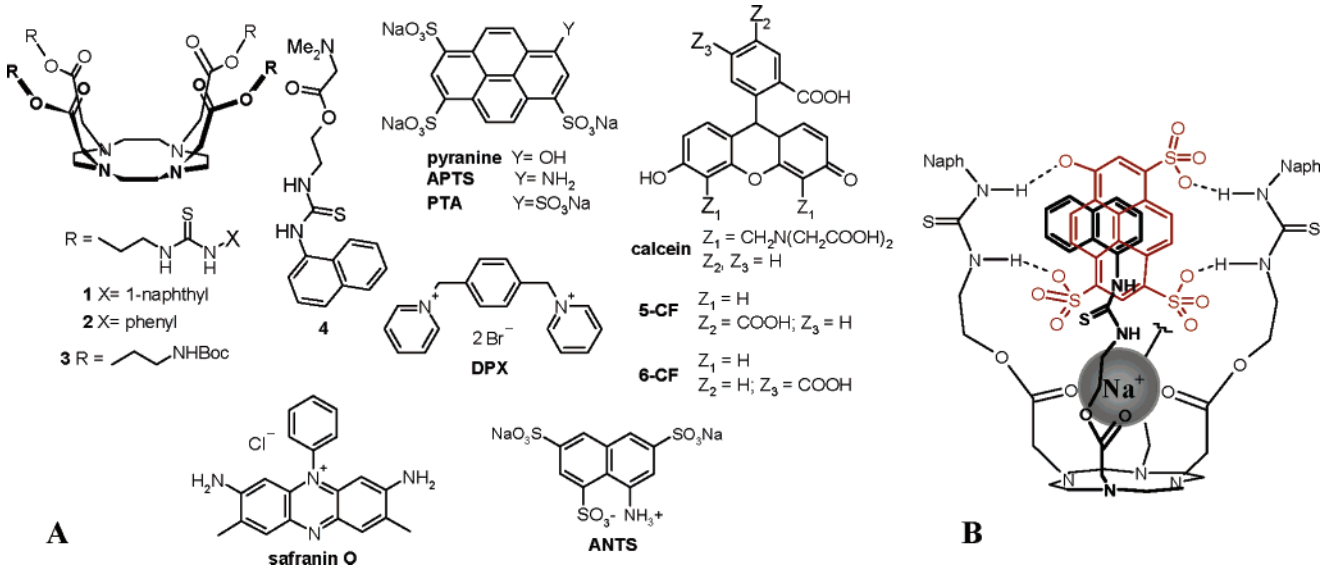

[a] The backside thiourea unit of cyclen **1** is truncated for clarity; this representation of binding mode is solely speculative and is given for pictorial purposes only.

Results and Discussion

Design of the Receptor. We reasoned that a compound capable of selective binding of pyranine (Chart 2) at micromolar concentrations, impermeable to the bilayer membrane, and capable of quenching of pyranine fluorescence would provide the basis for improved assays that do not rely on a high concentration of pyranine quencher. The structure of pyranine comprises a planar pyrene core and four peripheral anionic groups. It has been reported that cyclen tetraesters bind physiologically abundant Na^+, forcing all four ester termini to come into close proximity.[17] We speculated that if two of these termini would hydrogen-bond to pyranine sulfonates and phenolate and the two other termini would π-stack with pyranine's aromatic core, we would achieve a receptor for this dye. Additional stabilization of the complex is envisioned through the electrostatic interactions of the protonated cyclen scaffold with anionic sulfonates and the phenolate of pyranine. Cyclen **1** satisfied these requirements and was synthesized via a four-step procedure (Scheme S1, Supporting Information). The schematic representation of the envisioned binding mode for cyclen **1** and pyranine is shown on Chart 2B.

Pyranine−Cyclen 1 Complex Characterization. The first indication of interaction between cyclen **1** and pyranine dye was obtained from the extraction experiments. When a $CDCl_3$ solution of cyclen **1** was treated with an aqueous solution of pyranine, formation of precipitate was observed. Regardless of the pyranine and cyclen **1** mole ratios, the minor component was always almost completely removed from the solution phase upon extraction. The precipitate formed was soluble in DMSO-d_6, and the ^{1}H NMR spectrum of this DMSO solution has shown signals corresponding to pyranine and cyclen **1**. The chemical shifts of pyranine and cyclen **1** signals in DMSO were identical to those recorded for pyranine and cyclen **1** alone, suggesting that the complex was destroyed by this solvent. The integral ratios for signals of two compounds were independent of their mole ratios in the extraction series and corresponded to 1:1 complex stoichiometry.

To gain more information on the thermodynamics of the complexation process, a series of isothermal titration calorimetry (ITC) experiments were performed. The ITC experiments require substantial solubility of interacting components in the common solvent, although formation of a precipitate upon interaction is acceptable.[18] Cyclen **1** has a very limited solubility in water, therefore methanolic solutions were used instead. Both pyranine and cyclen **1** have a solubility of at least 15 mM in methanol which was suitable for ITC titrations. As with the extraction experiments, the addition of a methanolic solution of pyranine to cyclen **1** resulted in an extensive precipitate formation.

The formation of two distinct types of complexes was observed when a 10 mM solution of cyclen **1** was titrated into a 0.25 mM solution of pyranine in an ITC experiment (Figure 1). The assessed thermodynamic data for these complexes are summarized in Table 1. The first complex shows 1:1 stoichiometry, whereas the second complex corresponds to the overall 1:4 pyranine/cyclen **1** stoichiometry. These two complexes have different strengths and are driven by different thermodynamic forces. The originally formed 1:1 complex is 2 orders of magnitude stronger than the subsequently formed 1:4 complex. Whereas the formation of the 1:4 complex is an enthalpically driven process, the 1:1 complex formation is almost entirely an entropically driven process. The entropically driven 1:1 binding is consistent with the solvophobic effect most likely accompanying $\pi-\pi$ rather than hydrogen-bonding or electrostatic interactions.[19] A much weaker 1:4 complex formation is a mostly enthalpically driven process accompanied by a smaller positive entropy change. This second complexation step is probably due to the electrostatic and/or hydrogen-bonding

(17) (a) Shinoda, S.; Nishimura, T.; Tadokoro, M.; Tsukube, H. *J. Org. Chem.* **2001**, *66*, 6104−6108. (b) Nishimura, T.; Shinoda, S.; Tsukube, H. *Chirality* **2002**, *14*, 555−557.

(18) (a) Wu, J.; Du, F.; Zhang, P.; Khan, I. A.; Chen, J.; Liang, Y. *J. Inorg. Biochem.* **2005**, *99*, 1145−1154. (b) Sidorov, V.; Kotch, F. W.; El-Khouedi, M.; Davis, J. T. *Chem. Commun.* **2000**, 2369−2370. (c) Boots, J. W. P.; Chupin, V.; Killian, J. A.; Demel, R. A.; de Kruijff, B. *Biochim. Biophys. Acta* **1999**, *1420*, 241−251.

(19) (a) Nakamura, K.; Da, Y. Z.; Jikihara, T.; Fujiwara, H. *Bull. Chem. Soc. Jpn.* **1995**, *68*, 782−786. (b) Lin, F. Y.; Chen, W. Y.; Hearn, M. T. W. *Anal. Chem*. **2001**, *73*, 3875−3883.

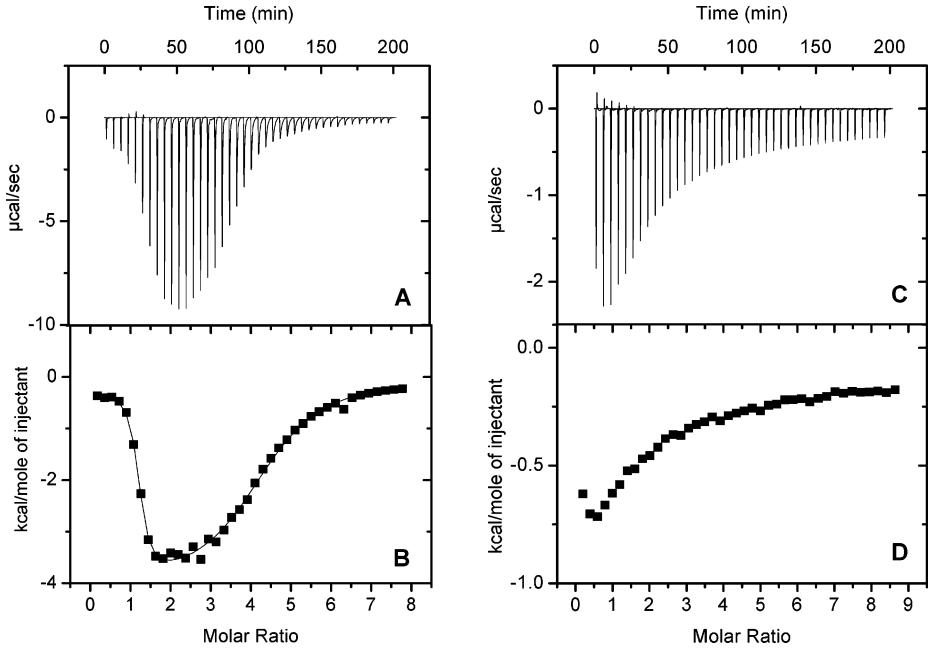

Figure 1. Microcalorimetric characterization of interactions of cyclen **1** with pyranine and calcein in methanol. (A) Raw data for the titration of a 0.25 mM solution of pyranine with a 10 mM solution of cyclen **1**. (B) Integrated data from (A), corrected by the heat of cyclen **1** dilution, normalized to moles of injectant and plotted as a function of cyclen **1**/pyranine ratios (solid squares). A continuous line represents the data fit in two sets of sites binding model. (C) Raw data for the titration of a 0.25 mM solution of calcein with a 10 mM solution of cyclen **1.** Note the difference in vertical scales for plots (A) and (C). (D) Integrated data from (C), corrected by the heat of cyclen **1** dilution, normalized to moles of injectant and plotted as a function of cyclen **1**/calcein ratios.

Table 1. Thermodynamic Parameters Assessed for the Complexation of Pyranine with Cyclen **1** in Methanol[a]

N^a	$K_a(M^{-1})$	ΔG (kcal/mol)	ΔH (kcal/mol)	$T\Delta S$ (kcal/mol)
1.28 ± 0.014	$(3.16 \pm 0.75) \times 10^6$	-8.87 ± 0.17	-0.41 ± 0.05	8.47
3.57 ± 0.050	$(1.46 \pm 0.12) \times 10^4$	-5.68 ± 0.05	-3.87 ± 0.08	1.81

[a] Number of binding sites for the individual complexation step obtained from the data fit to two sets of sites binding model.

interactions of cyclen **1** molecules with the initially formed 1:1 complex. Although the solvophobic effect plays a role in the 1:4 complex formation as well, the diminished entropy change likely stems from the decrease in the degrees of freedom for the large aggregate formed from several molecules. Noteworthy, no additional inflection points between 1:1 and 1:4 pyranine/cyclen **1** ratios were observed in the ITC plot, suggesting that the second binding process proceeds via a concerted cooperative mechanism.

^{1}H NMR analysis of the precipitate formed upon addition of an equimolar amount of cyclen **1** to pyranine in methanol revealed that these two compounds produced a 1:1.5 mixture. This ratio can be explained by the concurrent formation of a 1:1 complex (83%) and a 1:4 complex (17%). Clearly, the complexation of pyranine with cyclen **1** is a solvent-dependent process: whereas 1:1 complexes were formed from both aqueous and methanolic solutions, the enthalpically favored 1:4 complex was observed only for methanol, consistent with the fact that electrostatic and hydrogen-bonding interactions are weakened in water compared to less-polar methanol.[20] The fact that the complex between pyranine and cyclen **1** apparently does not form in a polar but not self-associated solvent such as DMSO[21,22] also supports the solvophobic effect as a primary driving force for the complex formation.

Evaluation of Cyclen 1 Affinity and Specificity to Pyranine under Near-Physiological Conditions. To be useful for kinetic biomembrane fluorometric assays, the pyranine receptor must (a) have high affinity to the dye under physiological conditions; (b) be impermeable to the membrane bilayer; (c) have fast kinetics of interaction with the dye; and (d) alter the fluorescence of the dye significantly.

The solubility of cyclen **1** in aqueous medium is very limited, and even if the binding to pyranine is strong, the capacity of cyclen **1** for binding with increasing amounts of the dye is limited by its concentration in the solution. We detected the solubility limit for cyclen **1** in a phosphate saline buffer (PBS, 100 mM NaCl, 10 mM P_i, pH = 6.4) through a series of UV−vis experiments where the absorbance of cyclen **1** solutions was plotted as a function of its concentration (Figure S6, Supporting Information). The saturation of absorbance was reached between 20 and 30 μM of cyclen **1** concentration. This concentration was ascribed to the limiting solubility of cyclen **1** in PBS. At concentrations of 40 μM and above, precipitation was visually observed.

(20) (a) Grawe, T.; Schrader, T.; Zadmard, R.; Kraft, A. *J. Org. Chem.* **2002**, *67*, 3755−3763. (b) Katsuta, S.; Ito, Y.; Kudo, Y.; Takeda, Y. *Inorg. Chim. Acta* **2005**, *358*, 713−719. (c) Hakem, I. F.; Lal, J.; Bockstaller, M. R. *Macromolecules* **2004**, *37*, 8431−8440.

(21) (a) Pang, Y. P.; Miller, J. L.; Kollman, P. A. *J. Am. Chem. Soc.* **1999**, *121*, 1717−1725. (b) Emseis, P.; Leverett, P.; Reddy, N.; Williams, P. A. *Inorg. Chim. Acta* **2003**, *355*, 144−150. (c) Mulski, M. J.; Connors, K. A. *Supramol. Chem.* **1995**, *4*, 271−278.

(22) No apparent complex formation between cyclen **1** and pyranine was observed in acetonitrile as well.

Table 2. Binding Constants and Maximal Fluorescence Loss Assessed for the Complexes of Pyrene-Based Dyes and Cyclen **1** from Fluorometric Titrations in PBS[a]

	HPTS	PTA	APTS	HPTS-**2**[b]
K_a (M^{-1})	$(2.6 \pm 0.3) \times 10^6$	$(2.1 \pm 0.5) \times 10^6$	$(7.7 \pm 1.0) \times 10^5$	$(9.2 \pm 1.3) \times 10^5$
I^{max}_{rel} (%)	90.9 ± 1.6	103 ± 4.7	99.3 ± 2.8	96 ± 3.0

[a] A 1:1 binding mode was assumed. [b] Binding parameters assessed for pyranine−cyclen **2** complex.

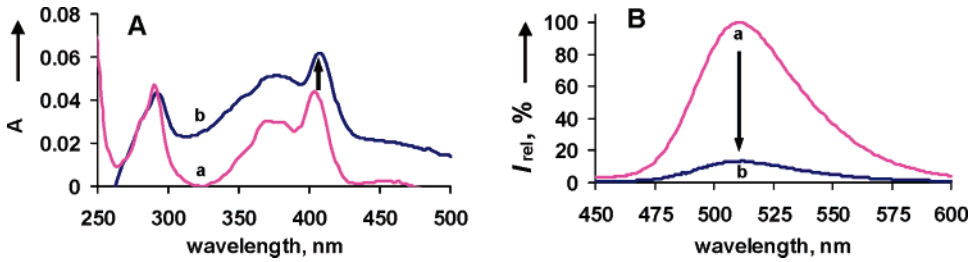

Figure 2. UV−vis (A) and fluorescence (B, ex = 405 nm) spectra for (a) 2.67 μM solution of pyranine in 1% of DMSO in PBS. PBS with the same amount of DMSO was used as a blank solution in UV−vis; (b) 2.67 μM pyranine, 10 μM cyclen **1** solution in 1% solution of DMSO in PBS. A 10 μM solution of cyclen **1** in 1% of DMSO in PBS was used as a blank in UV−vis. The arrow directions show the change of the property upon complexation.

Titration of pyranine with cyclen **1** in PBS demonstrated an extensive loss of the dye fluorescence (Figure S4, Supporting Information). This loss was insensitive to the presence of Cl^- and, surprisingly, to P_i.[23] The assessment of the binding constant gave an apparent value of $(2.6 \pm 0.3) \times 10^6$ M^{-1} (Table 2), meaning that low micromolar concentrations of cyclen **1** are sufficient to quench pyranine emission. Interestingly, the K_a value assessed for the pyranine−cyclen **1** complex in PBS from fluorometric titrations was very close to the K_a value determined by ITC for the 1:1 complexation step in methanol. Although receptors for pyranine of lower[24] or comparable affinity are known,[5d,25] to the best of our knowledge no fluorescence quenchers for pyranine, active at such low concentration, have been reported to date. The affinity of cyclen **1** to pyranine in aqueous medium compares favorably to that of the other artificial receptors for anionic substrates.[26] Importantly, the application of cyclen **1** to egg yolk phosphatidylcholine (EYPC) LUVs loaded with 100 μM PBS solution of pyranine did not result in a significant loss of pyranine fluorescence, showing that cyclen **1** is impermeable to the bilayer membrane.

The binding of pyranine to cyclen **1** in methanol and in the water/chloroform extraction experiments at high (millimolar) concentrations was always associated with the extensive complex precipitation. It was not clear whether the same precipitation is a leading cause of the fluorescence disappearance at nanomolar concentrations of pyranine. To determine the reason for this fluorescence loss, a parallel series of UV−vis and fluorometric experiments were performed. A PBS solution containing 20 μM of pyranine and 20 μM of cyclen **1** showed a decrease in both pyranine absorbance at $\lambda_{max} = 406$ nm and pyranine emission at 510 nm with excitation at 405 or 460 nm (Figure S5, Supporting Information). This result was inconclusive, as the loss of absorbance could be due to the complex precipitation or hypochromic shift induced by cyclen **1**. However, when the concentration of pyranine and cyclen **1** were reduced to 2.67 and 10 μM respectively, the fluorometric experiment still showed a loss of pyranine fluorescence, whereas the UV−vis experiment showed an increase in pyranine absorbance accompanied by a modest bathochromic shift (Figure 2). This hyperchromic shift cannot be due to the complex precipitation, and therefore it reflects the binding of cyclen **1** and pyranine in solution. We concluded that the solubility product K_{sp} for the pyranine complex in PBS is higher than 2.67×10^{-11} and is lower than 4×10^{-10}. The emission quenching observed in the fluorescence titration series with pyranine at 50 nM and cyclen **1** at up to 10 μM concentrations therefore corresponds to a concentration product of up to 5×10^{-13}, which is below the solubility product for this complex. We concluded that the fluorescence loss by pyranine in the titration experiments was due to the formation of a water-soluble complex, but not to the complex precipitation.

While the insolubility of a pyranine−cyclen **1** complex precluded its full structural characterization, a series of control experiments demonstrated the importance of all elements present in cyclen **1**. Thus, neither cyclen tetra-NH-Boc **3** nor the monomer **4** affected pyranine emission at concentrations up to 100 μM. These results suggest recognition of pyranine rather than a simple electrostatic interaction of pyranine with cyclen **1**, as well as the importance of four binding arms in cyclen **1**. With the solvophobic effect identified as a primary driving force for the complexation of pyranine by cyclen **1**, the cyclen tetraphenylthiourea **2** was expected to show a weaker binding to pyranine. Indeed, the assessed K_a value $(9.2 \pm 1.3) \times 10^5$ M^{-1}) for the cyclen **2**−pyranine complex was 3 times smaller than that for the cyclen **1**−pyranine complex.

To show specificity of cyclen **1** toward the pyranine structure, the affinity of cyclen **1** to several other dyes in PBS was evaluated. Four different categories of dyes were tested. The first category combines the pyrene-based 1,3,6,8-tetrasulfonic acid (PTA) and 8-aminopyrene-1,3,6-trisulfonic acid (APTS) with a topology similar to that of pyranine. The PTA molecule is decorated with four sulfonic groups in place of substituents of pyranine, whereas the amino group of the APTS molecule conceptually replaces the OH group of pyranine. The next

(23) (a) Gomez, D. E.; Fabbrizzi, L.; Licchelli, M.; Monzani, E. *Org. Biomol. Chem.* **2005**, *3*, 1495−1500. (b) Nishizawa, S.; Yokobori, T.; Kato, R.; Yoshimoto, K.; Kamaishi, T.; Teramae, N. *Analyst* **2003**, *128*, 663−669. (c) Buhlmann, P.; Nishizawa, S.; Xiao, K. P.; Umezawa, Y. *Tetrahedron* **1997**, *53*, 1647−1654.
(24) Atilgan, S.; Akkaya, E. U. *Tetrahedron Lett.* **2004**, *45*, 9269−9271.
(25) Ronan, D.; Sorde, N.; Matile, S. *J. Phys. Org. Chem.* **2004**, *17*, 978−982.
(26) (a) Snowden, T. S.; Anslyn, E. V. *Curr. Opin. Chem. Biol.* **1999**, *3*, 740−746. (b) Martinez-Manez, R.; Sancenon, F. *Chem. Rev.* **2003**, *103*, 4419−4476. (c) Sessler, J. L.; Camiolo, S.; Gale, P. A. *Coord. Chem. Rev.* **2003**, *240*, 17−55. (d) Ronan, D.; Sorde, N.; Matile, S. *J. Phys. Org. Chem.* **2004**, *17*, 978−982.

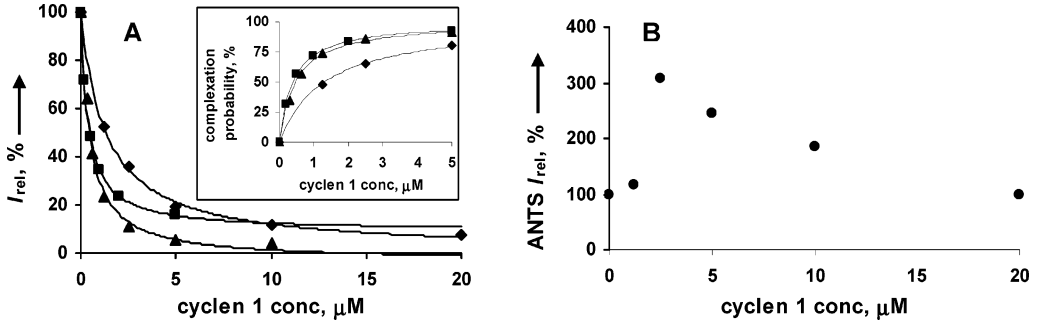

Figure 3. (A) Fluorometric titrations of 50 nM PBS solutions of pyranine (triangles, ex 405 nm, em 510 nm), PTA (squares, ex 376 nm, em 403 nm), and APTS (diamonds, ex 424 nm, em 503 nm) with cyclen **1**. Experimental data are normalized to the percentage of unbound dye fluorescence. Continuous lines represent best fits to a 1:1 binding model. Note that the three dyes show different extents of fluorescence loss upon binding to cyclen **1**. Inset shows the extent of complexation calculated for the data points from the main Figure 3A as a function of cyclen **1** concentration. The point shapes denote the same dyes as in the main Figure 3A. (B) Fluorometric titration of 50 nM ANTS (ex 365 nm, em 515 nm) with cyclen **1** in PBS. No fitting to a binding model was attempted.

category was represented by 8-aminonaphthalene 1,3,6-trisulfonate (ANTS). This dye features a naphthalene core in place of pyranine's pyrene and is decorated with the same periphery as the APTS molecule. The third category of dyes combines anionic fluorescein-based dyes 5-CF, 6-CF, and calcein. Whereas the electronic nature of the substituents in these dyes is similar to those found in pyranine, the central cores of these dyes lack pyranine's planarity and extended conjugation. Finally, the cationic dye safranin O was chosen as a negative control to demonstrate that the fluorescence loss was not due to a nonspecific quench. The test of binding for these model dyes was performed using fluorescence, UV−vis, and microcalorimetry titrations. The results of binding assays for selected dyes are summarized in Table 2.

Both APTS and PTA dyes produced complexes with cyclen **1** (Figure 3A). While the K_a value for the PTA−cyclen **1** complex in PBS was almost identical to that of the pyranine−cyclen **1** complex, a 3-fold drop in K_a value for the less-anionic APTS molecule was observed. This drop demonstrates the importance of electrostatic interactions in the cyclen **1**−pyranine complex.

The ANTS dye has demonstrated binding to cyclen **1** as well; however, the titration results were drastically different from those for pyranine, PTA, or APTS dyes (Figure 3B). While all three pyrene-based dyes gradually lost their fluorescence during the course of the titrations, the fluorescence of ANTS dye initially increased and reached a 3-fold maximum of the original fluorescence at the cyclen **1** concentration of 2.5 μM. Further increase of the cyclen **1** concentration resulted in a decrease of ANTS fluorescence, which reached its original value at a cyclen **1** concentration of 20 μM. Clearly, such binding behavior cannot be described using a 1:1 binding model.[27] Formation of bigger than 1:1 aggregates, complex precipitation, or the combination of both can account for such complexation behavior. The observed fluorescence loss of ANTS is not due to the increased optical density of the solution at the excitation wavelength, as this optical density never exceeded the value of 0.05.[28] Since the ANTS−cyclen **1** binding was not the main objective of the present study, no further attempt to clarify such binding behavior was undertaken.

For the third category of dyes comprising fluorescein derivatives, no apparent binding by cyclen **1** was detected at up to 20 μM concentrations by fluorometric and UV−vis titration experiments.[29] For calcein, the most anionic dye within this category, the possibility of binding was also tested by ITC in methanolic solution. These ITC experiments revealed small, compared to pyranine, gradually decreasing negative enthalpy of interaction without pronounced stoichiometric inflection points (Figure 1, parts C and D). This heat emission can be well explained by protonation of the basic cyclen **1** by the acidic calcein. The apparent absence of binding for fluorescein derivatives demonstrates the crucial importance of the planar conjugated core of the pyrene (and naphthalene)-based dyes for their recognition by cyclen **1**.

As expected, no binding of the cationic dye safranin O by cyclen **1** was detected by UV−vis and fluorometric experiments.

Applicability of Cyclen 1 to Biomembrane Assays. To validate the applicability of cyclen **1** to the membrane leakage assay, we performed experiments with the typical defect-forming peptide, melittin, and a typical ion channel forming peptide, gramicidin.[30] As expected, the pH-stat experiments on pyranine-loaded LUVs showed high, yet almost indistinguishable, activity of these peptides (Figure 4A). The application of these peptides to the same population of LUVs along with cyclen **1** clearly revealed the difference in the two peptides' mechanisms of action (Figure 4B). Whereas little loss of pyranine emission was observed for gramicidin (trace a), a significant loss of emission was observed for melittin (trace b) when cyclen **1** was applied to the extravesicular buffer. A steady fluorescence quench observed in the presence of melittin reflects the kinetics of pyranine release rather than the kinetics of cyclen **1**−pyranine complexation. Indeed, the experiment where melittin was injected first and cyclen **1** was added after 4 min revealed a rapid quench of fluorescence, suggesting that most of the dye had been released by that time (trace c). Both traces b and c are almost identical at longer times, indicating that the amount of released pyranine was independent of cyclen **1**.

(27) Connors, K. A. In *Binding Constants*; Wiley & Sons: New York, 1987; pp 161−168.
(28) Lakowicz, J. R. In *Principles of Fluorescence Spectroscopy*; Kluwer Academic/Plenum Publishers: New York, 1999; pp 54−56.
(29) 6-CF lost 9% of its fluorescence in the presence of 20 μM cyclen **1**. Some binding of 6-CF to cyclen **1** is possible; however, low solubility of cyclen **1** in PBS precluded accurate assessment of the binding constant. Data fitting into a 1:1 isotherm within the range of available cyclen **1** concentrations gave a value of 5×10^3 M^{-1} as a highest estimate for the K_a of the 6-CF−cyclen **1** complex.
(30) (a) Dempsey, C. E. *Biochim. Biophys. Acta* **1990**, *1031*, 143−161. (b) Finkelstein, A.; Andersen, O. S. *J. Membr. Biol.* **1981**, *59*, 155−171.

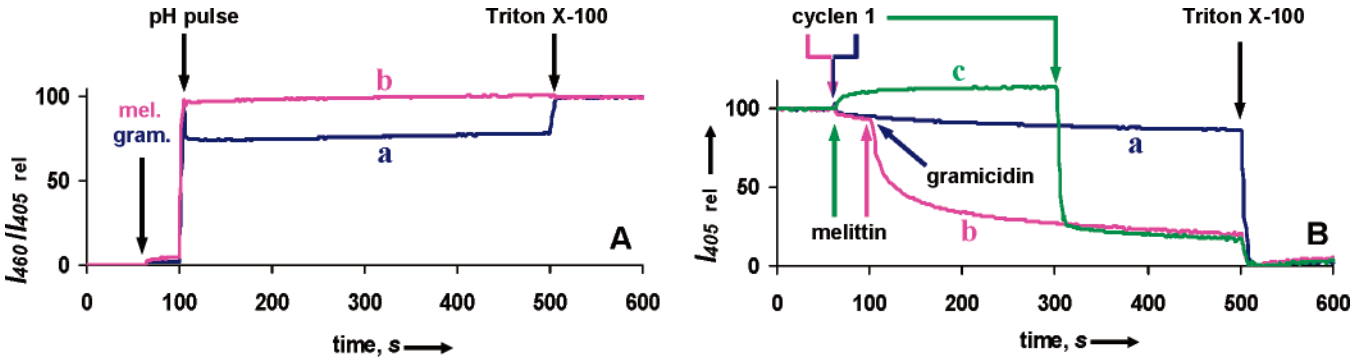

Figure 4. (A) pH-stat assays in the absence of cyclen **1** performed on pyranine-loaded LUVs with 1 μM gramicidin (a, blue trace) and 5 μM melittin (b, pink trace). I_{460}/I_{405} was monitored as function of time. (B) Membrane leakage assays performed on the same LUVs with cyclen **1**. I_{405} was monitored as function of time. Color code and time events: blue trace (a) 10 μM cyclen **1** at 60 s, 1 μM gramicidin at 100 s; pink trace (b) 10 μM cyclen **1** at 60 s, 5 μM melittin at 100 s; green trace (c) 5 μM melittin at 60 s, 10 μM cyclen **1** at 300 s. Termination at 500 s: 0.5% Triton X-100.

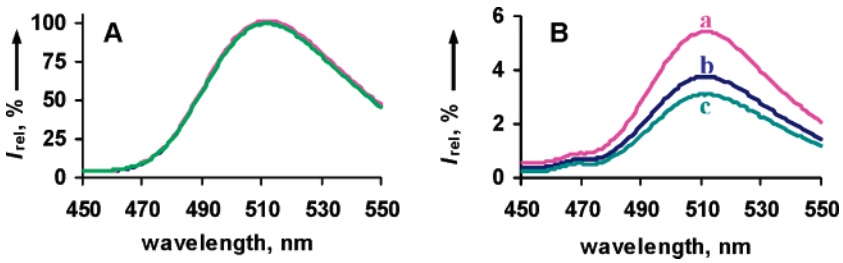

Figure 5. (A) Emission spectra (ex 405 nm) recorded for three sets of liposomes containing 0, 20, and 90 μM solutions of pyranine and suspended in the buffer containing 90 nM of pyranine. (B) Emission spectra for the same sets of liposomes after the treatment with cyclen **1**. The scale unit in (B) is the same as in (A). Color code for the traces in both (A) and (B): pink (a) LUVs containing 90 μM pyranine solution; blue (b) LUVs containing 20 μM pyranine solution; green (c) LUVs containing no pyranine.

Unfortunately, cyclen **1** has found only limited applicability in the detection of endovesiculation. Unlike with membrane leakage assay, where all the dye was entrapped in liposomes and any measurable change in fluorescence was sufficient for the event detection, the endovesiculation detection required a fluorescence quench of large amounts of extravesicular dye in the presence of small amounts of the dye entrapped in LUVs. Only the quenchers that suppress the fluorescence of the dye completely can be utilized in this assay. The high concentration of DPX used in the currently employed endovesiculation detection assay is due to the low affinity of DPX to pyranine. The assessed affinity of DPX to pyranine in PBS solution gave a K_a value of $(1.2 \pm 0.2) \times 10^3$ M^{-1}, which is 3 orders of magnitude lower than the K_a value for the pyranine−cyclen **1** complex formed under identical conditions. However, the ultimate quenching efficiency of DPX toward pyranine exceeds 99.7%,[15a] whereas the quenching efficiency of cyclen **1** is not that high. Our titration experiments showed that the cyclen **1**−pyranine complex has an intrinsic fluorescence of approximately 9% of the fluorescence of complex-free pyranine.

To increase the quenching efficiency of cyclen **1,** we adopted a new protocol for the detection of endovesiculation. Three sets of 600-nm EYPC LUVs containing 0, 20, and 90 μM solutions of pyranine in 100 mM HEPES/100 mM NaCl buffer (pH 7.1), respectively, were prepared and suspended in a 90 μM solution of pyranine in HEPES buffer. These three sets were used to mimic 0, 22, and 100% endovesiculation extent. A 20-μL aliquote of each population of liposomes was diluted with 2 mL of pyranine-free HEPES buffer and treated with 20 μL of a 4 mM solution of cyclen **1** in DMSO. Cyclen **1** was not fully soluble at this 40 μM concentration, and precipitate was formed. However, there was an apparent interaction of pyranine at the surface of microcrystals formed by cyclen **1,** resulting in more efficient removal of the dye from solution and fluorescence quench. Because of the noise and fluorescence produced by the precipitated cyclen **1**−pyranine complex, the solutions of LUVs were filtered through a cotton layer prior to the fluorometric experiments (Figure 5).

The emission spectra produced by these three sets of LUVs in the absence of cyclen **1** were almost indistinguishable due to the high extravesicular concentration of the dye (Figure 5A). The levels of the residual fluorescence for these sets of LUVs after the treatment with cyclen **1** were different and qualitatively consistent with the amounts of the dye entrapped inside (Figure 5B). LUVs containing no pyranine showed 3.1% fluorescence intensity in the absence of cyclen **1**. LUVs containing 20 and 90 μM solutions of pyranine showed 3.7% and 5.4% original fluorescence intensity, respectively. These results were reproducible with the accuracy of $\pm$20% when the time between the addition of cyclen **1** and solution filtration was fixed at 5 min. Longer incubations resulted in lower levels of fluorescence intensity, although the relative values were close to those observed at 5 min of incubation.

Even with the advantage of low quencher concentration, this new endovesiculation detection assay cannot replace the currently existing DPX-based assay for several reasons. First, an additional filtration step is required, which lowers the accuracy of the results. Second, there is a kinetic dependence of the fluorescence quench. Third, the results cannot be internally normalized after the filtration step.[31] Finally, the incomplete quench of the external pyranine emission drastically limits the sensitivity of the cyclen **1**-based assay. With all these disadvantages, the cyclen **1**-based assay can still be used as a control

to remove the ambiguity imposed by a high concentration of the quencher in the DPX-based assay.

The limitations in applicability of cyclen **1** to biomembrane assays arose from its low solubility and insufficient quenching efficiency. We plan to improve these characteristics in the future by covalently attaching DPX and poly(ethylene glycol) (PEG) units to the cyclen−thiourea core. These modifications should afford a pyranine receptor combining all features essential for membrane assays, and this is the focus of our ongoing study.

In conclusion, we have rationally designed and synthesized a pyranine receptor cyclen **1.** Cyclen **1** revealed a high affinity to pyranine dye under near-physiological conditions. Utilizing this affinity and the impermeability of cyclen **1** to the bilayer membrane, we have developed a new membrane leakage assay that is fully compatible with the pH-stat assay. Applying the methods described herein, it becomes possible to distinguish between ion transport and membrane leakage within a single set of experiments. We have also shown some limited applicability of cyclen **1** to the detection of endovesiculation and we are currently working on the synthesis of the pyranine-specific fluorescence quencher that is compatible with the endovesiculation assay.

Experimental Section

General. The ^{1}H NMR spectra were recorded on a Varian AS400 instrument operating at 400.130 MHz or a Varian Mercury instrument operating at 299.865 MHz. Chemical shifts are reported in ppm relative to the residual protonated solvent peak. The ^{13}C NMR spectra were recorded on the same instruments at 100.613 and 75.408 MHz, respectively, and chemical shift values are reported in ppm relative to the solvent peak. Both ^{1}H and ^{13}C spectra were taken in the same solvent and on the same instrument for each sample. The low-resolution mass spectra were recorded on a Micromass Q-TOF 2 instrument (Manchester, U.K.) using the electrospray technique (positive mode). The samples were introduced into a mass spectrometer using a flow rate of 10 μL/min, the needle voltage was set at 3500 V with ion source at 110 °C, and the cone voltage at 35 V. The high-resolution mass spectra were recorded on a LCMS-IT-TOF (Shimadzu Corporation, Columbia MD) instrument using the electrospray technique (positive mode). All spectrophotometric experiments were carried out on a Fluoromax 3 (Jobin-Yvon/Horriba) spectrophotometer. The dynamic light-scattering analysis of the liposome suspensions was carried out on the Malvern instrument (Malvern Zetasizer Nano Series, Malvern Instruments). Microcalorimetric titrations were performed using a VP-ITC microcalorimeter (MicroCal, LLC, Northampton MA), and the ORIGIN-7 software was used to calculate the binding constants and the enthalpy changes. The pH of solutions was monitored with a Corning 350 pH/ion analyzer, using a Ag/AgCl pH-sensitive electrode (Accumet). Chromatography was performed using 60−200-mesh silica purchased from Baker and 40−120-μm Sephadex G-75 purchased from Aldrich. Thin-layer chromatography was performed on Kieselgel 60 F254 and Uniplate Silica Gel GF silica-coated glass plates and visualized by UV and I_2. High-pressure extrusion was performed on the Avanti mini-extruder with a 0.1-μm polycarbonate membrane. All chemicals, solvents, and dyes were purchased from Aldrich, Sigma, Fluka, and Invitrogen. Egg yolk phosphatidylcholine was purchased from Avanti Polar Lipids.

(31) In the DPX-based assay, the fluorescence extent is normalized to the residual fluorescence observed after the lysis of LUVs by detergent. The filtration step in a cyclen **1**-based assay removes the quencher, and subsequent lysis does not result in a fluorescence change, whereas the external normalization with the residual fluorescence of pyranine-free LUVs lowers the accuracy of experiment.

Synthesis. The synthetic scheme for compounds **1**−**3** is shown in Scheme S1 of Supporting Information, and the synthetic procedure for compound **4** is shown in Scheme S2 of Supporting Information.

Bromoacetic Acid 2-*t*-Butoxycarbonylaminoethyl Ester 1a. *tert*-Butyl-*N*-(2-hydroxy ethyl) carbamate (4.5 g, 28 mmol) was dissolved in dichloromethane (30 mL), and triethylamine (3.9 mL, 28 mmol) was added. The mixture was stirred for 10 min at room temperature, and bromoacetyl bromide (3.15 mL, 36 mmol) was added dropwise within 5 min. The reaction mixture was stirred for 5 h at room temperature, the solvent was removed under reduced pressure, and the crude solid was purified by column chromatography (silica gel, CH_2Cl_2/EtOAc 4:6) to give 7.0 g of **2a** (25 mmol, 90%). ^{1}H NMR (300 MHz, DMSO-d_6, δ): 6.94 (t, 1 H, J = 5.7, 5.4 Hz), 4.11 (s, 2 H), 4.06 (t, 2 H, J = 5.7, 5.4 Hz), 3.15 (td, 2 H, J = 5.7, 5.7 Hz), 1.35 (s, 9 H); ^{13}C NMR (DMSO-d_6, δ): 167.7, 156.3, 78.5, 65.1, 39.3, 28.8, 27.9. MS (ESI) ([M+Na] $^+$): 304.01, calcd for $C_9H_{16}BrNO_4Na$ 304.02.

[4,7,10-Tris-(2-*tert*-butoxycarbonylamino-ethoxycarbonylmethyl)-1,4,7,10-tetraaza-cyclododec-1-yl]-acetic Acid 2-*tert*-butoxycarbonylamino-ethyl Ester (cyclen NH-Boc) 3. Cyclen (0.4 g, 2.3 mmol), sodium carbonate (2.19 g, 20.7 mmol), and bromoacetic acid 2-*tert*-butoxycarbonylamino ethyl ester (3.8 g, 13.8 mmol) were suspended in 20 mL of acetonitrile. The reaction mixture was stirred for 72 h at room temperature, and the solvent was removed under reduced pressure. The solid residue was purified by column chromatography (silica gel, $CH_3OH/CHCl_3$ 5:95) to afford 1.28 g of cyclen NH-Boc **3** (1.3 mmol, 56%). ^{1}H NMR (400 MHz, DMSO-d_6, δ): 6.89 (t, 4 H, J = 5.6, 6.0 Hz), 4.03 (br s, 8 H), 3.15 (br s, 8 H), 2.95−2.64 (br m, 16 H), 1.34 (s, 36 H); ^{13}C NMR (DMSO-d_6, δ): 174.0, 156.4, 78.5, 64.4, 55.4, 50.4, 28.8. MS (ESI, high-resolution) $[M+H]^+$, rel intensity 100.00: 977.5734, calcd for $C_{44}H_{81}BrN_8O_{16}$ 977.5765; $[M+Na]^+$, rel intensity 20.90: 999.5611, calcd for $C_{44}H_{80}BrN_8O_{16}Na$ 999.5585.

{4,7,10-Tris-[2-(3-naphthalen-1-yl-thioureido)-ethoxycarbonylmethyl]-1,4,7,10-tetraaza-cyclododec-1-yl}-acetic Acid 2-(3-naphthalen-1-yl-thioureido)-ethyl Ester 1. Cyclen NH-Boc **3** (1.0 g, 1 mmol) was dissolved in 10 mL of CH_2Cl_2, and trifluoroacetic acid (8 mL of 50% v/v solution in CH_2Cl_2) was added dropwise. The reaction mixture was stirred for 6 h at room temperature, and the solvent and excess of trifluoroacetic acid were removed under reduced pressure to afford crude deprotected cyclen **1b** tertrafluoroacetate (0.623 g, 0.603 mmol). Deprotected cyclen **1b** was reacted without further purification. The total amount obtained was dissolved in 15 mL of isopropyl alcohol, and 1-naphthyl isothiocyanate (1.5 g, 8 mmol) was added. After 15 min, triethylamine was added slowly to bring the pH to 9. The reaction mixture was stirred for 12 h at room temperature and then evaporated to dryness under reduced pressure. The crude solid was purified by column chromatography (silica gel, $CH_3OH/CHCl_3$ 5:95) to afford 0.26 g of pure cyclen **1** (0.2 mmol, 20% in two steps). ^{1}H NMR (400 MHz, DMSO-d_6, δ): 9.64 (s, 4 H), 7.92−7.81 (br m, 12 H), 7.51−7.41 (br m, 20 H), 4.17 (br s, 8 H), 3.72 (br s, 8 H), 2.92 (br s, 8 H), 2.63−2.63 (br m, 16 H); ^{13}C NMR (DMSO-d_6, δ): 182.8, 174.0, 134.6, 130.4, 128.8, 128.3, 127.5, 126.9, 126.6, 126.4, 125.8, 123.5, 63.6, 55.4, 50.8, 43.4. MS (ESI, high-resolution) $[M+H]^+$, rel intensity 100.00: 1317.4850, calcd for $C_{68}H_{77}N_{12}O_8$: 1317.4865; $[M+Na]^+$, rel intensity 36.12: 1339.4681, calcd for $C_{68}H_{76}N_{12}O_8Na$ 1339.4684.

{4,7,10-Tris-[2-(3-phenyl-thioureido)-ethoxycarbonylmethyl]-1,4,7,10-tetraaza-cyclododec-1-yl}-acetic Acid 2-(3-phenyl-thioureido)-ethyl Ester 2. This compound was synthesized from cyclen NH-Boc **3** (0.6 g, 0.61 mmol) and phenyl isothiocyanate (0.6 mL, 5 mmol) according to the procedure described for the synthesis of cyclen **1**. The isolated yield of cyclen **2** was 0.12 mmol, 23%. ^{1}H NMR (400 MHz, DMSO-d_6, δ): 9.62 (br s, 4 H), 7.91 (br s, 4 H), 7.34−7.26 (br m, 16 H), 7.10−7.06 (t, 4 H), 4.22 (br s, 8 H), 3.73 (br s, 8 H), 2.94 (br s, 8 H), 2.67−2.63 (br m, 16 H); ^{13}C NMR (DMSO-d_6, δ): 181.4, 174.0, 139.7, 129.3, 124.9, 123.7, 63.8, 55.5, 50.8, 43.1. MS (ESI) ([M+Na]$^+$): 1139.3, calcd for $C_{52}H_{68}N_{12}O_8Na$ 1139.40.

1-(2-Hydroxy-ethyl)-3-naphthalen-1-yl-thiourea 4a. This compound was synthesized according to the literature.[32] 2-Ethanolamine (0.18 mL, 2.7 mmol) was dissolved in 6.5 mL of EtOAc, and 1-naphthyl isothiocyanate (0.502 g, 2.7 mmol) was added. The reaction mixture was stirred for 20 min at room temperature. The white precipitate that was formed was washed with ethyl acetate, filtered, and purified by column chromatography (silica gel, EtOAc/CH_2Cl_2 9:1). Final recrystallization of the product from toluene gave 0.538 g of **4a** (2.19 mmol, 81%). ^{1}H NMR (DMSO-d_6, 25 °C, δ): 9.65 (s, 1 H), 7.95−7.91 (m, 1 H), 7.88−7.80 (m, 2 H), 7.56−7.46 (m, 5 H), 4.71 (s, 1 H), 3.52−3.50 (br d, 4 H, J = 6 Hz); ^{13}C NMR (DMSO-d_6, δ): 182.6, 135.1, 134.6, 130.4, 128.8, 127.1, 126.8, 126.3, 125.6, 123.4, 59.9, 47.3. MS (ESI) ([M+H]$^+$): 247.8, calcd for $C_{13}H_{14}N_2OS$ 246.08.

Dimethyaminoacetic Acid 2-(3-naphthalen-1-yl-thioureido)-ethyl Ester 4. To a solution of *N*,*N*-dimethyl glycine (103 mg, 1 mmol) in 10 mL of CH_2Cl_2, 1,1′-carbonyldiimidazole (162 mg, 1 mmol) was added. The reaction mixture was stirred for $3^1/_2$ h at room temperature, then 1-(2- hydroxy-ethyl)-3-naphthyl-thiourea (198 mg, 0.8 mmol) was added, and the reaction was stirred for another 12 h at room temperature. The solvent was evaporated under reduced pressure, and the residual solid was partitioned in chloroform/water. The organic layer was separated, and the solvent was removed under reduced pressure. The crude product was purified by column chromatography (silica gel, CH_3-OH/EtOAc 3:97) to give pure monomer **4** as a white solid (67 mg, 0.202 mmol, 25%). ^{1}H NMR (300 MHz, DMSO-d_6, δ): 9.74 (s, 1 H), 7.96−7.92 (m, 1 H), 7.87−7.81(m, 2 H), 7.57−7.41 (m, 5 H), 4.14 (t, 2 H, J = 5.6 Hz), 3.67 (td, 2 H, J = 5.5, 5.4 Hz), 3.09 (s, 2 H), 2.20 (s, 6 H); ^{13}C NMR (DMSO-d_6, δ): 182.7, 170.8, 134.7, 130.5, 128.8, 127.6, 126.9, 126.9, 126.4, 125.9, 123.5, 62.6, 59.9, 45.2, 43.6. MS (ESI, high-resolution) ([M+H]$^+$): 332.1408, calcd for $C_{17}H_{22}N_3O_2S$ 332.1427.

Liposome Preparation for pH-Stat and Membrane Leakage Assay. Egg yolk L-α-phosphatidylcholine (EYPC ethanol solution, 60 μL, 79 μmol) was dissolved in a $CHCl_3$/MeOH mixture, the solution was evaporated under reduced pressure, and the resulting thin film was dried under high vacuum for 2 h. The lipid film was hydrated for 40 min in 1.2 mL of sodium phosphate buffer (10 mM sodium phosphate, pH = 6.4, 100 mM NaCl,) containing 100 μM pyranine. During hydration, the suspension was submitted to three freeze−thaw cycles (dry ice/acetone, water at room temperature). The resulting suspension of large multilamellar vesicles (1 mL) was submitted to high-pressure extrusion at room temperature. As judged by the dynamic light scattering analysis, 21 extrusions through a 0.1-μm polycarbonate membrane afforded a suspension of LUVs with an average diameter of 130 nm. The LUV suspension was separated from the extravesicular dye by size-exclusion chromatography (SEC) (stationary phase: Sephadex G-75, mobile phase: pyranine-free sodium phosphate buffer of the same composition) and diluted with the same sodium phosphate buffer to give a stock solution with a lipid concentration of 11 mM (assuming 100% of lipid was incorporated into liposomes).

Liposome Preparation for Endovesiculation Detection Assay. LUVs for the endovesiculation detection were prepared analogously to those for the membrane leakage assay, except that the 100 mM HEPES/100 mM NaCl buffer (pH 7.1) containing pyranine at 0−90 μM concentrations was used instead of PBS for lipid hydration and the extrusion was carried out using 1-μm polycarbonate membrane. The DLS analysis of the final LUV suspension revealed a 600-nm average diameter of liposomes.

pH-Stat Transport Assays. In a typical experiment, 100 μL of pyranine-loaded LUVs (stock solution) was suspended in 1.9 mL of the symmetric pyranine-free buffer and placed into a thermostated spectrophotometric cell. The suspension of liposomes was gently stirred throughout the entire course of the experiment. The emission of pyranine at 510 nm was monitored with concurrent excitation at 405 and 460 nm. The emission and excitation slits of the spectrophotometer were set at 5 nm, time increments were set at 2 s, and the integration time was set at 0.5 s. The temperature of the spectrophotometric cell was set at 25 °C. During the experiment, 20 μL of a 0−100 μM DMSO solution of gramicidin or 0−500 μM aqueous solution of melittin was added through the injection port, followed by injection of 21 μL of 0.5 M aqueous NaOH. Addition of NaOH resulted in a pH increase of approximately 1 pH unit in the extravesicular buffer, as established by separate pH monitoring. Maximum possible changes in dye emission were obtained at the end of each experiment by lysis of the liposomes with detergent (40 μL of 25% aqueous Triton X-100). The final transport trace was obtained as a ratio of the emission intensities monitored at 460 and 405 nm and was normalized to 100% of transport.

Membrane Leakage Assays. The stock solution of the same LUVs as used in the pH-stat assays (100 μL) was suspended in 1.9 mL of the symmetric pyranine-free buffer and placed into a thermostated spectrophotometric cell. The instrumental settings were the same as in the pH-stat transport experiments. The suspension of liposomes was gently stirred throughout the course of the experiment. The emission of pyranine at 510 nm was monitored with excitation wavelength at 405 nm. During the experiment, 20 μL of a 0−1 mM solution of cyclen **1** in DMSO was injected into the suspension of LUVs, followed by the injection of 20 μL of the same solution of ionophore (gramicidin or melittin) as used in the pH-stat assays. The incubation time between injections of cyclen **1** and peptide was 40 s. When necessary, the sequence of injections was inverted, and the incubation time for the suspension of LUVs with peptide was increased up to 240 s. Maximal possible changes in the dye emission were obtained at the end of each experiment by lysis of LUVs with detergent (40 μL of 25% aqueous Triton X-100). The traces were normalized to 100% of the emission change of pyranine.

Microcalorimetric Titrations. The ITC titrations were carried out at 25 °C using 1.423 mL of a methanolic solution of titrated compound in the sample cell and the same amount of pure methanol in the reference cell. In each experiment, a total of 40 injections of constant volume (7 μL) of the titrant solution was made into the sample cell. The injections were separated by a lag time of 300 s. The heat change associated with the dilution of titrant in the injection series was assessed from independent experiments, where the titrant solution of the same concentration was injected into the pure solvent. The integrated data were corrected by the amount of heat evolved from the dilution of titrant, and the mole ratios were corrected by the dilution of components associated with the volume change during an experiment.

Fluorometric Titration of Pyranine with Cyclen 1. The fluorometric titration of pyranine with cyclen **1** shown in Figure S4 of Supporting Information. In a typical experiment, an aqueous solution (2 mL) containing 50 nM pyranine, 100 mM NaCl, and 10 mM $Na_xH_{3-x}PO_4$ (x = 1,2; pH 6.4) was placed into a thermostated spectrophotometric cell set at 25 °C. The solution was gently stirred during the experiment. Prior to the spectrophotometric recording, 20 μL of 0−500 μM solution of cyclen **1** in DMSO was added. The emission spectra were recorded with the excitation wavelength 405 nm. The recording was performed immediately after the addition of cyclen **1** and repeated after 30 min. Most of the fluorescence loss occurred instantly upon the addition of cyclen **1**. No further change of emission was observed at times longer than 30 min. For the accurate assessment of the binding constant, the emission maxima at 510 nm recorded after a 30-min delay time were used for the binding isotherm fitting. Binding constant and the maximum emission loss with the confidence interval values were computed using the homemade nonlinear regression curve-fitting program. The 1:1 binding model was used.

Fluorometric Experiments with Control Compounds and Dyes. The titration of pyranine's solutions with the control compounds was performed analogously to that with cyclen **1,** except that the concentrations of cyclen NH-Boc **3** and monomer **4** in these experiments were varied in the range of 0−100 μM and the concentration of cyclen **2**

(32) Qian, X.; Liu, F. *Tetrahedron Lett.* **2003**, *44*, 795−799.

was varied in the range of 0−20 μM. The titration of PTA, APTS, ANTS, calcein, 5-CF, 6-CF, and safranin O with cyclen **1** was identical to that of pyranine. The control dyes were kept at 50 nM concentration, whereas the concentration of cyclen **1** in the titration series was varied in the range of 0−20 μM. Table S1 of Supporting Information summarizes the instrumental settings for the fluorometric monitoring of the dyes. No detectable change in the emission of calcein and 5-CF was observed, whereas 9% fluorescence loss was observed for 6-CF in the presence of 20 μM cyclen **1**.

UV−Vis Titrations. The spectra of the dyes were recorded for the solutions in 1% of DMSO in PBS with 1% DMSO in PBS used as blank. For the spectra of the dyes in the presence of cyclen **1**, the solution of cyclen **1** in 1% of DMSO in PBS was used as a blank.

Acknowledgment. This work was supported by the generous VCU startup fund to V.S. and the Jeffress Memorial Trust. We thank Prof. Nicholas Farrell for use of his ITC, Prof. Sarah Rutan for critical reading, and Robert Everley for high-resolution MS analysis. We are indebted to an anonymous reviewer for extremely helpful suggestions.

Note Added after ASAP Publication: In the version published on the Internet September 27, 2005, Tables 1 and 2 contain production errors which confuse the meaning of the data. Tables 1 and 2 are correct in the version published September 28, 2005, and in the print version.

Supporting Information Available: Synthetic and spectroscopic data, fluorometric titrations. This material is available free of charge via the Internet at http://pubs.acs.org.

JA052397I